



## OPEN Differential tumor protein expression at follicular lymphoma diagnosis reveals dysregulation of key molecular pathways associated with histological transformation

Marie Hairing Enemark<sup>1,2</sup>, Katharina Wolter<sup>1</sup>, Trine Engelbrecht Hybel<sup>1,2</sup>, Maja Dam Andersen<sup>1</sup>, Emma Frasez Sørensen<sup>1,2</sup>, Linnea Meier Hindkaer<sup>1</sup>, Kristina Lystlund Lauridsen<sup>3</sup>, Charlotte Madsen<sup>1</sup>, Trine Lindhardt Plesner<sup>4</sup>, Stephen Hamilton-Dutoit<sup>3</sup>, Bent Honoré<sup>5</sup> & Maja Ludvigsen<sup>1,2</sup>✉

Follicular lymphoma (FL) is the most common low-grade lymphoma. Despite its indolent nature, FL carries an inherent risk of histological transformation (HT) to a more aggressive lymphoma. Existing biomarkers are insufficient to predict HT, indicating the need for more robust biological predictors. Previously, we used mass spectrometry-based proteomics to identify differentially expressed proteins in diagnostic FLs with and without subsequent HT. This study sought to further investigate identified proteins in transformation of FL, generally acting in important cellular pathways such as (i) apoptosis (BID), (ii) cell cycle (CDC26, CDK6, SRSF1, SRSF2), (iii) GTPase signaling (IQGAP2, MEK1), (iv) cytoskeletal rearrangement and cellular migration (ACTB, CD11a, MMP9, SEPT6), and (v) immune processes (CD81, IgG, MPO, PIK3AP1). We analyzed pre-therapeutic samples from 48 FL patients, either non-transforming FL (nt-FL,  $n = 30$ ) or subsequently-transforming FL (st-FL,  $n = 18$ ), the latter with histologically-confirmed transformation after their initial FL diagnosis. Paired high-grade lymphomas (tFL,  $n = 18$ ) from the time of transformation were also analyzed. We used immunohistochemistry and digital image analysis to quantify protein levels. In all five pathway classes, several proteins were differentially expressed between either the diagnostic nt-FL and st-FL samples, or between the paired st-FL and tFL samples ( $p < 0.05$ ). Interestingly, we found correlation between expression levels of several proteins, indicating a complex involvement between several pathways. Differential expression of most proteins was also associated with shorter transformation-free survival ( $p < 0.05$ ). These findings emphasize underlying differences in FL biology predictive of subsequent transformation, highlighting deregulation of important interconnected cellular pathways.

**Keywords** Follicular lymphoma, Histological transformation, Proteomics

The research was funded with grants from Department of Clinical Medicine, Aarhus University, the Karen Elise Jensen Foundation, Merchant Einar Willumsen's Memorial Foundation, the Danish Lymphoma Group, a donation from Peter and Alice Madsen, Knud and Edith Eriksen's Memorial Foundation, Eva and Henry Fränkel's Memorial Foundation, Raimond and Dagmar Ringgård-Bohn's Foundation, Butcher Max Wörzner and wife Wörzner's Memorial Grant, Master Carpenter Jørgen Holm and wife Elisa f. Hansen's Memorial Grant, A.P. Møller Foundation for the Advancement of Medical Sciences, Dagmar Marshall's Foundation, and Farmer of "Ølufgård" Peder Nielsen Kristensens Memorial Foundation.

<sup>1</sup>Department of Hematology, Aarhus University Hospital, Aarhus, Denmark. <sup>2</sup>Department of Clinical Medicine, Aarhus University, Aarhus, Denmark. <sup>3</sup>Department of Pathology, Aarhus University Hospital, Aarhus, Denmark. <sup>4</sup>Department of Pathology, Copenhagen University Hospital, Copenhagen, Denmark. <sup>5</sup>Department of Biomedicine, Aarhus University, Aarhus, Denmark. ✉email: majlud@rm.dk

## Introduction

Follicular lymphoma (FL) represents the most prevalent indolent entity within non-Hodgkin lymphomas. The development of FL involves intricate steps, with a pivotal event being the t(14;18) translocation<sup>1,2</sup>. While indolent in its nature, FL is generally considered incurable, and regardless of the therapeutic approach applied, there is an inherent risk of histological transformation (HT) into a more aggressive lymphoma histology, most commonly diffuse large B-cell lymphoma (DLBCL), at a rate of 2–3% per year<sup>1,2</sup>. While the mechanisms behind HT remain incompletely understood, it is believed to arise from sub-clonal populations that have adeptly evaded, neutralized, or co-opted the immune system, necessitating early detection and a comprehensive understanding of the underlying biology<sup>3,4</sup>. Although baseline clinical and patient features such as age, the follicular lymphoma international prognostic index (FLIPI), performance status, and the presence of B symptoms can offer valuable insights into disease prognosis<sup>3,5,6</sup>, none of the prevailing clinicopathological features or biomarkers presently offer a dependable prediction of the risk of transformation. Thus, identifying new biological predictors is imperative. FL tumor cells reside in a permissive non-malignant tumor microenvironment (TME), and identification and characterization of the TME has revealed its importance, the microenvironmental composition being intricately linked to prognosis and risk of HT<sup>7–11</sup>. As such, the TME may hold information on novel therapeutic markers. By targeting the TME, it may be possible not only to directly attack the tumor cells, but also to modulate the microenvironment, rendering it immunocompetent or hostile to tumor growth<sup>12</sup>.

We previously performed a hypothesis-generating large-scale mass spectrometry (MS)-based proteomics study which identified a broad selection of proteins differentially expressed in diagnostic lymphoma biopsies from patients with and without subsequent transformation. A total of five proteins all involved in apoptotic regulation was further investigated in tissue surroundings by an immunohistochemical approach, revealing a predictive role on subsequent transformation. In addition, the identified differentially expressed proteins influence various other important cellular pathways<sup>13</sup>. Thus, this proteomic assessment provided the initial grounds for our hypothesis that a variety of biological processes are altered in the HT process, either by the malignant cells or the surrounding TME, already at the time of FL diagnosis, and that these may be correlated with subsequent risk of HT. Based on this proteomic analysis, functionally relevant alterations could be roughly grouped into five major pathway classes: (i) apoptosis, (ii) cell cycle, (iii) GTPase signaling, (iv) cytoskeletal arrangement and cellular migration, and (v) processes of the immune system. In the present study, we sought to evaluate expression levels in situ of fifteen proteins known to act in these pathway classes, to investigate the revealed potential disturbances of these cellular pathways in transformation of FL<sup>13</sup>.

## Patients and methods

### Patient cohort

Immunohistochemical evaluation of selected proteins was performed on pre-therapeutic formalin-fixed, paraffin-embedded (FFPE) lymphoma samples from 48 FL patients. Patients were diagnosed with FL grade 1–3 A at Aarhus University Hospital, Denmark, between 1990 and 2015<sup>13</sup>. These included 30 non-transforming FL (nt-FL) patients who had no record of transformation with at least ten years of follow up, as well as 18 subsequently-transforming FL (st-FL) patients with histologically-confirmed transformation to DLBCL or FL grade 3B, at least six months after the primary FL diagnosis. This threshold in time was set to exclude cases of discordant/composite lymphomas. In addition, for the 18 st-FL patients, paired high-grade transformed samples (transformed FL, tFL) from the time of transformation were also analyzed. All biopsies were reviewed by two experienced hematopathologists (SJHD and TLP) and classified according to the 2017 update of the WHO Classification of Tumours of the Haematopoietic and Lymphoid Tissues<sup>2</sup>. Clinicopathological data on all patients were obtained from the Danish Lymphoma Registry<sup>14,15</sup>. Both clinicopathological and immunohistochemical data on other putative biological markers in this cohort have been published previously<sup>7,13,16–20</sup> (Table 1). The study was approved by the Danish National Committee on Health Research Ethics (1–10–72–276–13) and the Danish Data Protection Agency (1–16–02–407–13) and was conducted in accordance with the Declaration of Helsinki. Due to the retrospective nature of the study, informed consent was waived by the Danish Ethics Committee and the Danish Data Protection Agency.

### Immunohistochemical staining

Proteins selected for immunohistochemical evaluation were  $\beta$ -actin (ACTB), BH3 interacting-domain death agonist (BID), integrin alpha L (CD11a), cluster of differentiation 81 (CD81), cell division cycle 26 (CDC26), cyclin-dependent kinase 6 (CDK6), immunoglobulin G (IgG), IQ motif-containing GTPase-activating protein 2 (IQGAP2), dual specificity mitogen-activated protein kinase kinase 1 (MEK1), matrix metalloproteinase 9 (MMP9), myeloperoxidase (MPO), phosphoinositide 3-kinase adapter protein 1 (PIK3AP1), septin 6 (SEPT6), serine/arginine-rich splicing factor 1 (SRSF1), and serine/arginine-rich splicing factor 2 (SRSF2). These were all identified in the previous MS-based proteomics study<sup>13</sup>, and widely covered the five pathway classes: (i) apoptotic regulation (BID), (ii) cell cycle progression (CDC26, CDK6, SRSF1, SRSF2), (iii) GTPase signaling (IQGAP2, MEK1) (iv) cytoskeletal rearrangement and cellular migration (ACTB, CD11a, MMP9, SEPT6), and (v) immune processes (CD81, IgG, MPO, PIK3AP1).

Immunohistochemical staining was performed on 4  $\mu$ m FFPE sections using the Ventana Benchmark Ultra automated staining system (Ventana Medical Systems, Oro Valley, Arizona) as previously described<sup>13</sup>. Detailed information of heat-induced epitope retrieval, primary antibody dilution, and incubation times is described in Table S1. Visualization was performed using the OptiView DAB IHC Detection Kit (Ventana, 760–700) with nuclear counterstaining by hematoxylin. Sections of appendix, tonsil, liver, and pancreas were included on all slides as positive and negative controls<sup>13</sup>.

Characteristics	All n = 48 n (%)	nt-FL n = 30 n (%)	st-FL n = 18 n (%)	p-value
Sex				
Male	23 (48)	13 (43)	10 (56)	NS
Female	25 (52)	17 (57)	8 (44)	
Age at FL diagnosis				
Median	54	54	53	NS
Range	35–76	35–76	40–74	
Ann Arbor stage				
I-II	15 (31)	14 (47)	1 (6)	<b>0.003</b>
III-IV	31 (65)	15 (50)	16 (89)	
Unknown	2 (4)	1 (3)	1 (6)	
Unknown	2 (4)	1 (3)	1 (6)	
FLIPI				
Low	19 (40)	16 (53)	3 (17)	0.088
Intermediate	19 (40)	11 (37)	8 (44)	
High	6 (13)	1 (3)	5 (28)	
Unknown	4 (8)	2 (6)	2 (11)	
LDH-elevation				
Yes	2 (4)	1 (3)	1 (6)	NS
No	42 (88)	27 (90)	15 (83)	
Unknown	4 (8)	2 (6)	2 (11)	
B-symptoms				
Yes	11 (23)	5 (17)	6 (33)	NS
No	34 (71)	24 (80)	10 (56)	
Unknown	3 (6)	1 (3)	2 (11)	
Performance score				
< 2	36 (75)	25 (83)	11 (61)	NS
≥ 2	9 (29)	4 (13)	5 (28)	
Unknown	3 (6)	1 (3)	2 (11)	
Bone marrow involvement				
Yes	14 (29)	7 (23)	8 (44)	NS
No	28 (58)	20 (67)	8 (44)	
Unknown	6 (13)	4 (13)	2 (11)	
Anemia				
Yes	4 (8)	1 (3)	3 (17)	NS
No	41 (85)	28 (93)	13 (72)	
Unknown	3 (6)	1 (3)	2 (11)	
FL histology				
FL grade 1–2	41 (85)	25 (83)	16 (89)	NS
FL grade 3 A	7 (15)	5 (17)	2 (11)	

**Table 1.** Patients' clinicopathological features The level of significance for the entire paper is defined in the methods section as  $p < 0.05$ .

## Digital image analysis

Stained slides were scanned at a magnification of x20 using the Hamamatsu Nanozoomer 2.0HT scanner (Hamamatsu, Shizouka, Japan). Expression levels of all biomarkers were quantified using Visiopharm Integrator System (Visiopharm A/S, Hoersholm, Denmark), as previously described<sup>13</sup>. Regions of interest (ROI) were outlined on each digitized tissue section, excluding distinct areas of non-lymphoid tissue and technical artefacts in order to make the samples more comparable<sup>13</sup>. Expression levels were quantified as area fractions (AFs), defined as the stained area normalized to the total area within the ROI<sup>13</sup>. ACTB, BID, CD81, CDC26, CDK6, IgG, MPO, PIK3AP1, SEPT6, and SRSF1 expression levels were calculated on AFs of all positive staining, while CD11a, IQGAP2, MEK1, MMP9, and SRSF2 were calculated on AFs of strong-intensity staining. Intrafollicular regions were manually outlined guided by a consecutive parallel tissue section stained with PAX5 to identify B cell areas in the biopsies<sup>7,13,16</sup>. Since MPO staining showed little or no positive staining within follicles, quantification of this marker was not performed exclusively in intrafollicular areas. For some markers, insufficient tissue availability resulted in exclusion of up to six patients, Table 2. This reduction did not affect the overall cohort characteristics.

## Statistical analysis

Statistical analyses were performed as previously described<sup>13</sup>. P-values below 0.05 were considered statistically significant. Statistical analyses were performed using R Statistical Software (version 4.1.3).

## Results

### Patients

The patient cohort comprised 48 patients, including 23 males and 25 females with a relatively low median age at diagnosis of 54 years (range 35–76), Table 1. At the time of diagnosis, st-FL patients presented with more advanced Ann Arbor stage ( $p = 0.003$ ) and showed, accordingly, a trend towards higher FLIPI risk scores ( $p = 0.088$ ) than nt-FL patients. Otherwise, clinicopathological features were comparable between the two patient groups, Table 1.

Biomarker		All n (%)	nt-FL n (%)	st-FL n (%)	p-value		All n (%)	nt-FL n (%)	st-FL n (%)	p-value
<b>(i) Apoptotic regulation</b>										
<b>BID</b> n = 47	All section High Low	16 (34) 31 (66)	7 (23) 23 (77)	9 (53) 8 (47)	0.082	Intrafollicular High Low	22 (47) 25 (53)	11 (37) 19 (63)	11 (65) 6 (35)	NS
<b>(ii) Cell cycle regulation</b>										
<b>CDC26</b> n = 48	All section High Low	15 (31) 33 (69)	6 (20) 24 (80)	9 (50) 9 (50)	0.064	Intrafollicular High Low	19 (40) 29 (60)	9 (30) 21 (70)	10 (56) 8 (44)	NS
<b>CDK6</b> n = 48	All section High Low	14 (29) 34 (71)	5 (17) 25 (83)	9 (50) 9 (50)	<b>0.022</b>	Intrafollicular High Low	20 (42) 28 (58)	9 (30) 21 (70)	11 (61) 7 (39)	0.070
<b>SRSF1</b> n = 48	All section High Low	13 (27) 35 (73)	3 (10) 27 (90)	10 (56) 8 (44)	<b>0.002</b>	Intrafollicular High Low	13 (27) 35 (73)	5 (17) 25 (83)	8 (44) 10 (56)	<b>0.049</b>
<b>SRSF2</b> n = 45	All section High Low	12 (27) 33 (73)	12 (41) 17 (59)	0 (0) 16 (100)	<b>0.003</b>	Intrafollicular High Low	16 (36) 29 (64)	15 (52) 14 (48)	1 (6) 15 (94)	<b>0.003</b>
<b>(iii) GTPase signaling</b>										
<b>IQGAP2</b> n = 42	All section High Low	23 (55) 19 (45)	19 (76) 6 (24)	4 (24) 13 (76)	<b>0.001</b>	Intrafollicular High Low	19 (45) 23 (55)	15 (60) 10 (40)	4 (24) 13 (76)	<b>0.029</b>
<b>MEK1</b> n = 48	All section High Low	23 (48) 25 (52)	12 (40) 18 (60)	11 (61) 7 (29)	NS	Intrafollicular High Low	26 (54) 22 (46)	15 (50) 15 (50)	11 (61) 7 (39)	NS
<b>(iv) Cytoskeletal rearrangement and cellular migration</b>										
<b>ACTB</b> n = 47	All section High Low	14 (30) 33 (70)	3 (10) 26 (90)	11 (61) 7 (29)	<b>&lt; 0.001</b>	Intrafollicular High Low	12 (26) 35 (74)	3 (10) 26 (90)	9 (50) 9 (50)	<b>0.005</b>
<b>CD11a</b> n = 48	All section High Low	16 (33) 32 (67)	9 (30) 21 (70)	7 (29) 11 (61)	NS	Intrafollicular High Low	35 (73) 13 (27)	7 (23) 23 (77)	12 (67) 6 (33)	<b>0.008</b>
<b>MMP9</b> n = 48	All section High Low	11 (23) 37 (77)	2 (7) 28 (93)	9 (50) 9 (50)	<b>&lt; 0.001</b>	Intrafollicular High Low	27 (56) 21 (44)	12 (40) 18 (60)	15 (83) 3 (17)	<b>0.006</b>
<b>SEPT6</b> n = 48	All section High Low	24 (50) 24 (50)	15 (50) 15 (50)	9 (50) 9 (50)	NS	Intrafollicular High Low	37 (79) 10 (21)	26 (87) 4 (13)	11 (65) 6 (35)	NS
<b>(v) Immune processes</b>										
<b>CD81</b> n = 42	All section High Low	21 (50) 21 (50)	17 (65) 9 (35)	4 (25) 12 (75)	<b>0.025</b>	Intrafollicular High Low	12 (29) 29 (70)	10 (38) 16 (62)	2 (13) 13 (87)	NS
<b>IgG</b> n = 46	All section High Low	26 (57) 20 (43)	19 (68) 9 (32)	7 (29) 11 (61)	NS	Intrafollicular High Low	21 (46) 25 (54)	12 (43) 16 (57)	9 (50) 9 (50)	NS
<b>MPO</b> n = 48	All section High Low	15 (31) 33 (69)	5 (17) 25 (83)	10 (56) 8 (44)	<b>0.009</b>	Intrafollicular	- -	- -	- -	
<b>PIK3AP1</b> n = 48	All section High Low	25 (52) 23 (48)	18 (60) 12 (40)	7 (29) 11 (61)	NS	Intrafollicular High Low	15 (31) 33 (69)	14 (47) 16 (53)	1 (6) 17 (94)	<b>0.003</b>

**Table 2.** Immunohistochemical expression of the selected proteins Dichotomous high/low biomarker expression was determined as the optimal cutoff value in AFs from TFS analyses based on ROC analyses and Youden's index. P-values were calculated from a chi-square test or Fisher's exact test. The level of significance for the entire paper is defined in the methods section as  $p < 0.05$ .

### Expression levels of selected proteins acting in all five pathways show differences between nt-FL and st-FL

Proteins for evaluation were selected in order to investigate the potential disturbances in five pathway classes in FL transformation, namely (i) apoptotic regulation, (ii) cell cycle progression, (iii) GTPase signaling, (iv) cytoskeletal rearrangement and cellular migration, and (v) immune processes. Notably, the immunohistochemical staining showed differential staining patterns of proteins within all pathway classes of both neoplastic and non-neoplastic cellular subsets in the lymphoma samples. Immunohistochemical staining of ACTB, CD81, PIK3AP1, and SEPT6 showed diffuse cytoplasmic staining of both neoplastic and non-neoplastic cells in the TME, with positive staining more densely located within intrafollicular areas, Figs. 1, 2, 3, 4 and 5; Table 2. This was also true CDK6 which showed, in addition to cytoplasmic staining, some positivity in nuclei, Fig. 2B. In addition to intrafollicular staining, IgG also showed specific interfollicular cellular subsets with intensively positive staining, Fig. 5B. Conversely, the diffuse cytoplasmic positive staining seen with IQGAP2 and CD11a was more densely

Figure 1

## (i) Apoptotic regulation

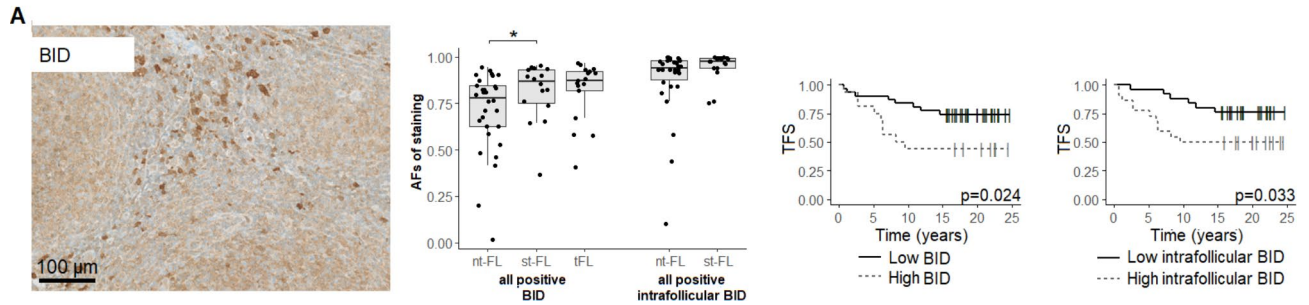


**Fig. 1.** Expression of proteins and transformation-free survival according to proteins involved in apoptotic regulation. Left: Representative image of lymphoma tissues immunohistochemically stained for BID. Visualized at x20. Middle: Expression levels are calculated as AFs identified by immunohistochemical staining in whole-biopsy and intrafollicular areas. Right: associations between TFS in whole-biopsy and intrafollicular expression levels, respectively, of BID (cutoff AF = 0.8556 and AF = 0.962). \* $p < 0.05$ ; \*\* $p < 0.01$ ; \*\*\* $p < 0.001$ . AF, area fraction; nt-FL, non-transforming FL; st-FL, subsequently-transforming FL; tFL, transformed FL; TFS, transformation-free survival.

located in interfollicular areas, Figs. 3A and 4B. An interfollicular localization was also evident for MMP9 and MPO stainings, although these were generally restricted to more specific cellular subsets, with some cells also showing positive nuclear MPO staining, Figs. 4C and 5C. Nuclear staining were also seen for CDC26, SRSF1, and SRSF2 which exhibited similar staining profiles, all being present in both intrafollicular and interfollicular areas, Fig. 2A, C, D. Interestingly, BID and MEK1 both showed diffuse weak expression in both intrafollicular and interfollicular areas, but also exhibited strongly positive specific cellular subsets, mainly located interfollicularly, Figs. 1A and 3B; Table 2.

At the time of initial diagnosis, disturbances were observed in all five pathway classes. st-FL samples had significantly higher expression levels of BID ( $p = 0.048$ ), CDK6 ( $p = 0.046$ ), ACTB ( $p = 0.005$ ), MMP9 ( $p = 0.002$ ), and MPO ( $p = 0.012$ ) compared with nt-FL samples, while elevated SRSF1 levels were trending ( $p = 0.068$ ), Figs. 1, 2, 3, 4 and 5. Conversely, st-FL samples had lower expression levels of IQGAP2 ( $p = 0.022$ ) than nt-FL samples, Fig. 3A. At the time of transformation, expression levels were significantly decreased in high-grade tFL samples compared with st-FL samples with regard to ACTB ( $p = 0.001$ ), CD11a ( $p = 0.001$ ), MEK1 ( $p = 0.027$ ), MMP9 ( $p = 0.004$ ), and SRSF2 ( $p = 0.021$ ), Figs. 1, 2, 3, 4 and 5. Conversely, the expression of CD81 was trending towards increased levels in tFL ( $p = 0.058$ ), Fig. 5A. When quantifying expression levels exclusively localized within intrafollicular areas, a significant difference between nt-FL and st-FL samples was observed in stains for MMP9 ( $p = 0.005$ ) and PIK3AP1 ( $p = 0.022$ ), while BID ( $p = 0.052$ ) and IQGAP2 ( $p = 0.061$ ) retained trending differential expression patterns, Figs. 1, 2, 3, 4 and 5.

### The expression levels of several proteins showed correlations indicating a complex interplay in the cellular homeostasis

Expression levels of several markers showed significant correlations to each other as shown in Table 3, suggesting that the five pathway classes are intricately interconnected in multiple ways. Interestingly, while most proteins showed positive correlations to each other, most correlations to SRSF2 were negative associations, including the apoptotic protein BID, the cellular adhesion molecule CD11a, the cell cycle regulators CDC26, CDK6, and SRSF1, as well as the immune cell component MPO. The only two positive correlations to SRSF2 expression were Ras GTPase-activator IQGAP2 and the MAPK/ERK-activator MEK1. Notably, all other correlations of the latter two markers were also negative associations, Table 3. Taken together, these results indicate an intricate interplay of proteins and pathways underlying FL biology.

The pathways could further be related to clinical presentation and other clinicopathological features, Table 4. Markers involved in cytoskeletal rearrangement and cellular migration, as well as processes of the immune system, were negatively associated with bone marrow involvement, namely CD11a expression ( $p = 0.036$ ;  $\rho = -0.33$ ), CD81 expression ( $p = 0.002$ ;  $\rho = -0.49$ ), IgG levels ( $p = 0.005$ ;  $\rho = -0.43$ ), and SEPT6 levels (trending;  $p = 0.059$ ;  $\rho = -0.29$ ), suggesting lower expression levels correlated to the presence of involvement of the bone marrow. Conversely, MMP9 levels showed a strong positive association to bone marrow involvement ( $p = 0.001$ ;  $\rho = 0.48$ ). Expression of MMP9 was also negatively correlated to lymphocyte counts ( $p = 0.014$ ;  $\rho = -0.38$ ). Moreover, FLIPI risk scores were also positively correlated with the cytoskeletal/cellular migration markers MMP9 ( $p = 0.002$ ;  $\rho = 0.46$ ), and borderline ACTB ( $p = 0.051$ ;  $\rho = 0.30$ ), as well as the cell cycle regulator CDK6 ( $p = 0.028$ ;  $\rho = 0.33$ ). In addition, markers driving the FLIPI risk score showed correlations, including LDH levels being associated with CD11a ( $p = 0.047$ ,  $\rho = -0.30$ ), hemoglobin levels being associated with CDK6 ( $p = 0.037$ ,  $\rho = 0.31$ ), Ann Arbor stage being associated with CDK6 ( $p = 0.003$ ,  $\rho = 0.42$ ), MMP9 ( $p < 0.001$ ,  $\rho = 0.47$ ), and SEPT6 ( $p = 0.048$ ,  $\rho = -0.29$ ), as well as age being negatively associated with MMP9 ( $p = 0.014$ ,  $\rho = -0.35$ ) and MPO ( $p = 0.048$ ,  $\rho = -0.29$ ). Furthermore, female gender was associated with higher expression of the apoptotic

Figure 2

## (ii) Cell cycle progression

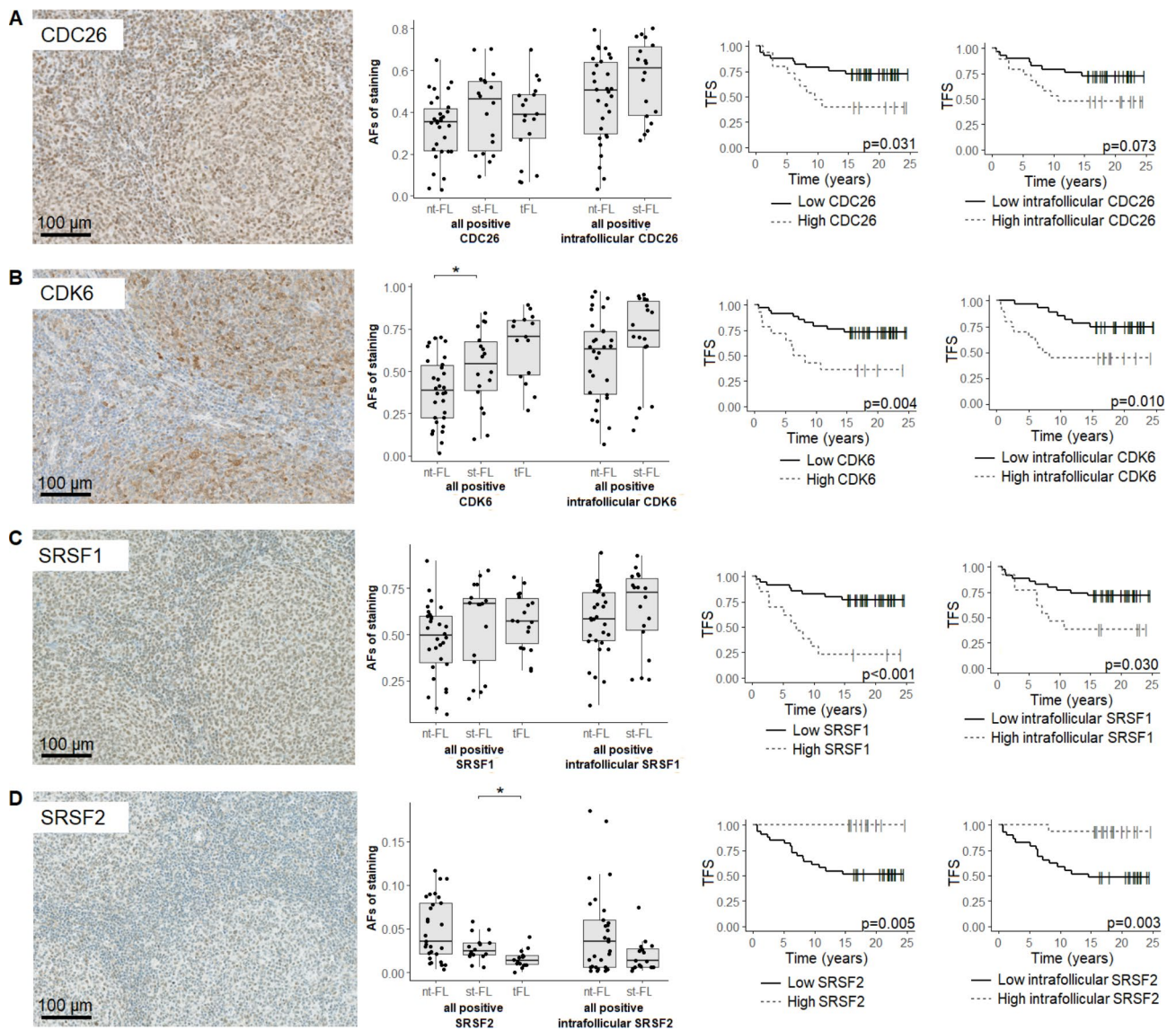


**Fig. 2.** Expression of proteins and transformation-free survival according to proteins involved in cell cycle progression. Left: Representative images of lymphoma tissues immunohistochemically stained for (A) CDC26, (B) CDK6, (C) SRSF1, and (D) SRSF2. Visualized at x20. Middle: For each protein, expression levels are calculated as AFs identified by immunohistochemical staining in whole-biopsy and intrafollicular areas. Right: associations between TFS in whole-biopsy and intrafollicular expression levels, respectively, of CDC26 (cutoff AF = 0.4462 and AF = 0.5883), CDK6 (cutoff AF = 0.5874 and AF = 0.6903), SRSF1 (cutoff AF = 0.6638 and AF = 0.7519) and SRSF2 (cutoff AF = 0.3083 and AF = 0.5216). \*  $p < 0.05$ ; \*\*  $p < 0.01$ ; \*\*\*  $p < 0.001$ . AF, area fraction; nt-FL, non-transforming FL; st-FL, subsequently-transforming FL; tFL, transformed FL; TFS, transformation-free survival.

regulator BID ( $p = 0.041$ ;  $\rho = 0.30$ ) and immune regulator PIK3AP1 ( $p = 0.019$ ;  $\rho = 0.34$ ), with cell cycle regulator CDC26 trending ( $p = 0.055$ ;  $\rho = 0.27$ ). Lastly, MPO expression also showed a positive correlation to increasing FL grade ( $p = 0.017$ ;  $\rho = 0.34$ ).

#### Dysregulated expression of proteins acting in all five pathway classes were associated with inferior transformation-free survival

Factors from all five pathway classes showed their impact on transformation-free survival (TFS), with high expression levels of ACTB ( $p < 0.001$ ), BID ( $p = 0.024$ ), CDC26 ( $p = 0.031$ ), CDK6 ( $p = 0.004$ ), MMP9 ( $p < 0.001$ ), MPO ( $p = 0.004$ ), and SRSF1 ( $p < 0.001$ ), as well as low expression levels of CD81 ( $p = 0.022$ ), IQGAP2

## (iii) GTPase signaling

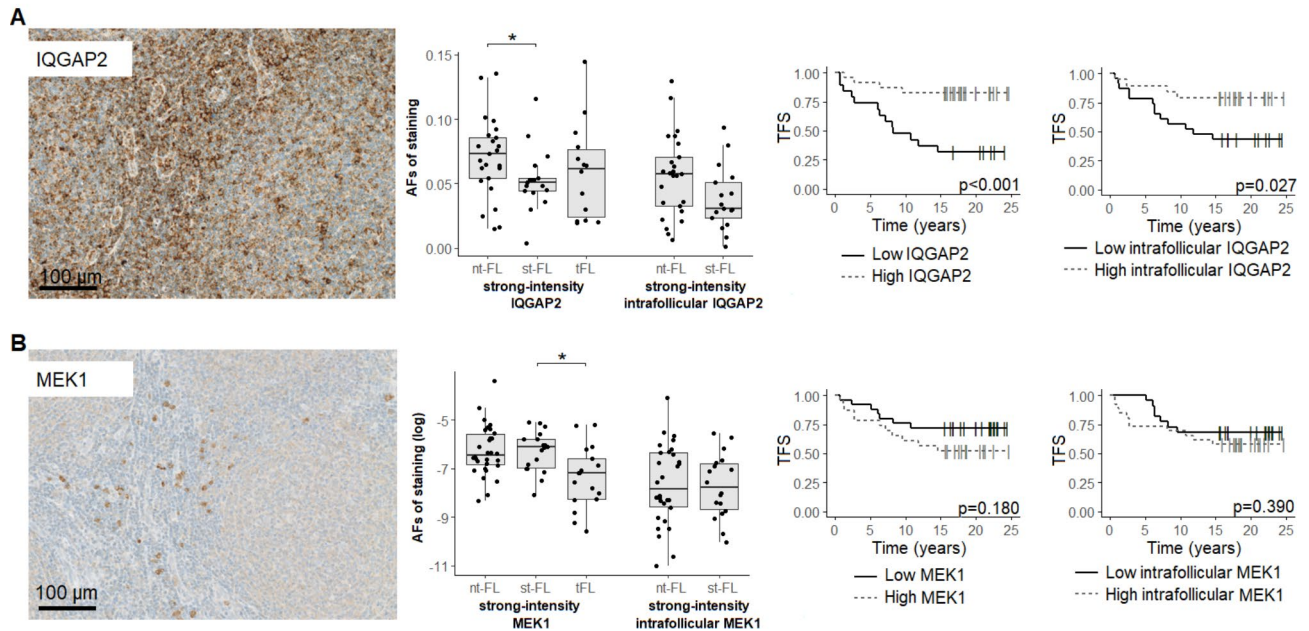


**Fig. 3.** Expression of proteins and transformation-free survival according to proteins involved in GTPase signaling. Left: Representative images of lymphoma tissues immunohistochemically stained for (A) IQGAP2 and (B) MEK1. Visualized at  $\times 20$ . Middle: For each protein, expression levels are calculated as AFs identified by immunohistochemical staining in whole-biopsy and intrafollicular areas. Right: associations between TFS in whole-biopsy and intrafollicular expression levels, respectively, of IQGAP2 (cutoff AF = 0.0539 and AF = 0.0548) and MEK1 (cutoff AF = 0.0019 and AF = 0.0003). \*  $p < 0.05$ ; \*\*  $p < 0.01$ ; \*\*\*  $p < 0.001$ . AF, area fraction; nt-FL, non-transforming FL; st-FL, subsequently-transforming FL; tFL, transformed FL; TFS, transformation-free survival.

( $p < 0.001$ ), SRSF2 ( $p = 0.005$ ), and IgG levels (trending;  $p = 0.053$ ) being associated with significantly shorter TFS, Figs. 1, 2, 3, 4 and 5. When analyzing exclusively intrafollicular areas, high expression of ACTB ( $p = 0.002$ ), BID ( $p = 0.033$ ), CDK6 ( $p = 0.010$ ), MMP9 ( $p = 0.003$ ), SRSF1 ( $p = 0.030$ ), and SRSF2 ( $p = 0.003$ ) were associated with significantly inferior TFS, while CDC26 expression levels were only trending ( $p = 0.073$ ). The same was evident for low intrafollicular levels of IQGAP2 ( $p = 0.027$ ), PIK3AP1 ( $p = 0.006$ ), SEPT6 ( $p = 0.047$ ), and SRSF2 ( $p = 0.003$ ), Figs. 1, 2, 3, 4 and 5.

## Discussion

We investigated five cellular pathway classes previously demonstrated to be important in transformation of FL<sup>13</sup>, evaluating the immunohistochemical expression levels of fifteen selected proteins acting in this broad spectrum of important pathways, including (i) apoptosis, (ii) cell cycle, (iii) GTPase signaling, (iv) the cytoskeleton and cellular migration, and (v) the immune system. All fifteen proteins were previously identified as differentially expressed in FL biopsies by an explorative hypothesis-generating MS-based proteomics assessment<sup>13</sup>. Here we show, that at time of FL diagnosis, proteins acting in apoptosis, and cytoskeletal rearrangement and cellular migration pathways, in particular, were dysregulated at primary FL diagnosis in samples that subsequently underwent transformation, as shown by increased ACTB, BID, and MMP9 expression levels in st-FL samples compared with nt-FL samples. In addition, the impact of all five pathway classes on transformation of FL was shown by differential protein expression levels, either distributed throughout the tumor tissues, or restricted to intrafollicular areas. Proteins were associated with significantly inferior TFS rates, including ACTB, BID, CD81, CDK6, IQGAP2, MMP9, MPO, PIK3AP1, SRSF1, and SRSF2. While still explorative in its nature, our study allows a more detailed definition of pathways and proteins that may be important in the pathogenesis of histological transformation in FL. As a result, we believe that increased research focus on biomarkers in FL that identify such expression signatures and elucidate their clinical significance, may clarify the pathophysiological mechanisms that underlie the disease. This in turn, may potentially pave the way for improved therapeutic strategies in the disease.

Importantly, in the present study, we analyzed whole-biopsy sections, however restricted to a ROI only including lymphoid tissue, thus taking non-neoplastic cells of the TME into account in the biomarker analysis, while excluding larger areas of connective tissue, vessels, fatty tissue etc. Indeed, the TME has shown its impact in FL, with a number of previous studies correlating non-neoplastic immune cell infiltrates, and cellular interplay, to overall clinical behavior<sup>7,9,11,21</sup>. As shown by the staining reactions, several proteins were indeed expressed

## (iv) Cytoskeletal rearrangement and cellular migration

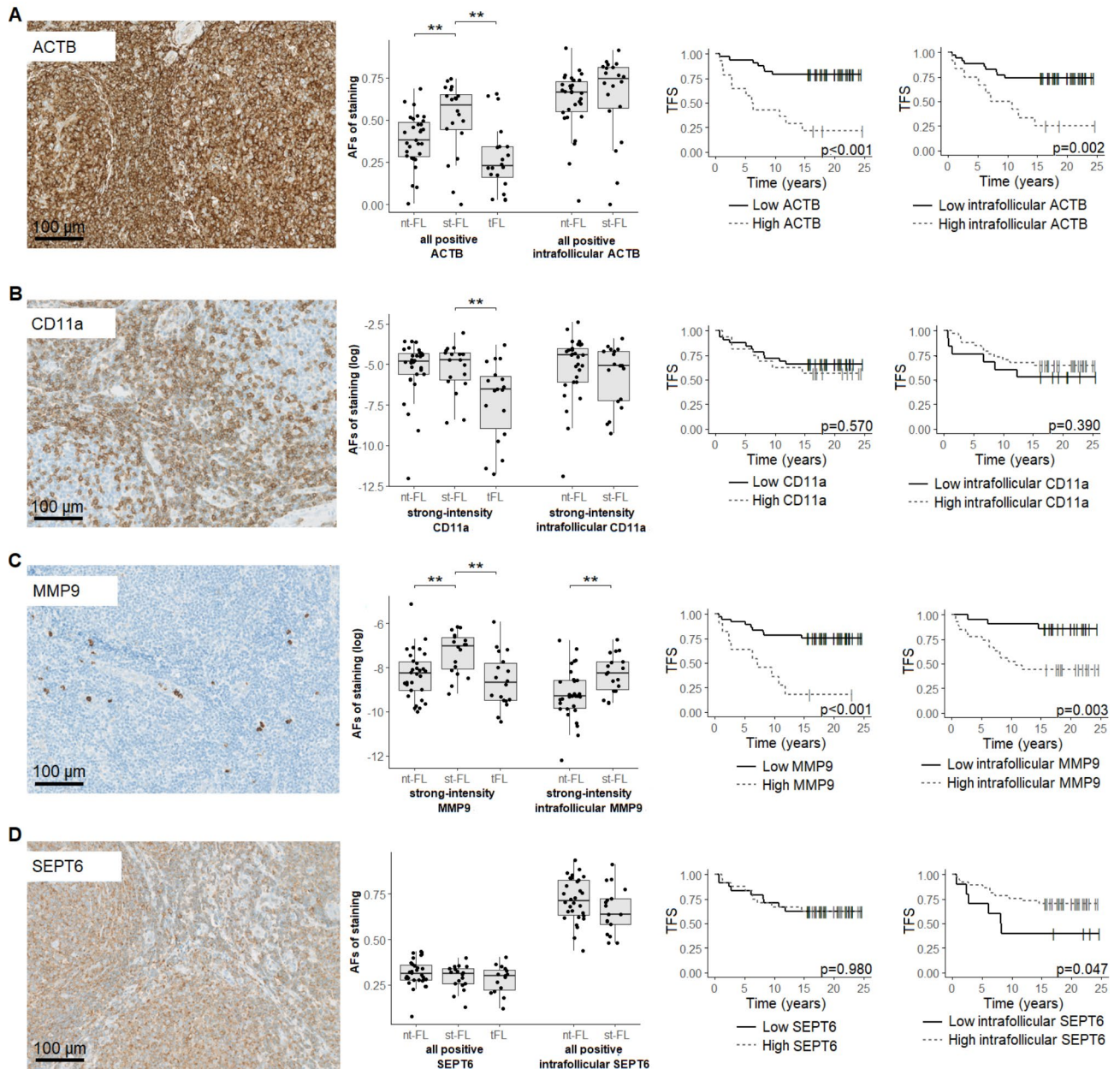


**Fig. 4.** Expression of proteins and transformation-free survival according to proteins involved in cytoskeletal rearrangement and cellular migration. Left: Representative images of lymphoma tissues immunohistochemically stained for (A) ACTB, (B) CD11a, (C) MMP9, and (D) SEPT6. Visualized at x20. Middle: For each protein, expression levels are calculated as AFs identified by immunohistochemical staining in whole-biopsy and intrafollicular areas. Right: associations between TFS in whole-biopsy and intrafollicular expression levels, respectively, of ACTB (cutoff AF = 0.534 and AF = 0.7678), CD11a (cutoff AF = 0.0125. And AF = 0.002), MMP9 (cutoff AF = 0.0009 and AF = 0.0001), and SEPT6 (cutoff AF = 0.3092 and AF = 0.6003). \*  $p < 0.05$ ; \*\*  $p < 0.01$ ; \*\*\*  $p < 0.001$ . AF, area fraction; nt-FL, non-transforming FL; st-FL, subsequently-transforming FL; tFL, transformed FL; TFS, transformation-free survival.

by infiltrating cells in the tumor microenvironment. Thus, possible transformation-promoting effects by such proteins may be attributed to, not just the malignant tumor cells, but also the tumor bystander cells. While several proteins were interesting in the context of HT, the well-known tumor heterogeneity of FL was also evident, the expression levels of several markers varying within each patient group. From large-scale MS-based proteomics to targeted antibody-based immunohistochemistry, we aimed for evaluation of proteins using a more clinically applicable methodology, which would be a prerequisite for the prospective use of putative predictive markers in



## (v) Immune processes

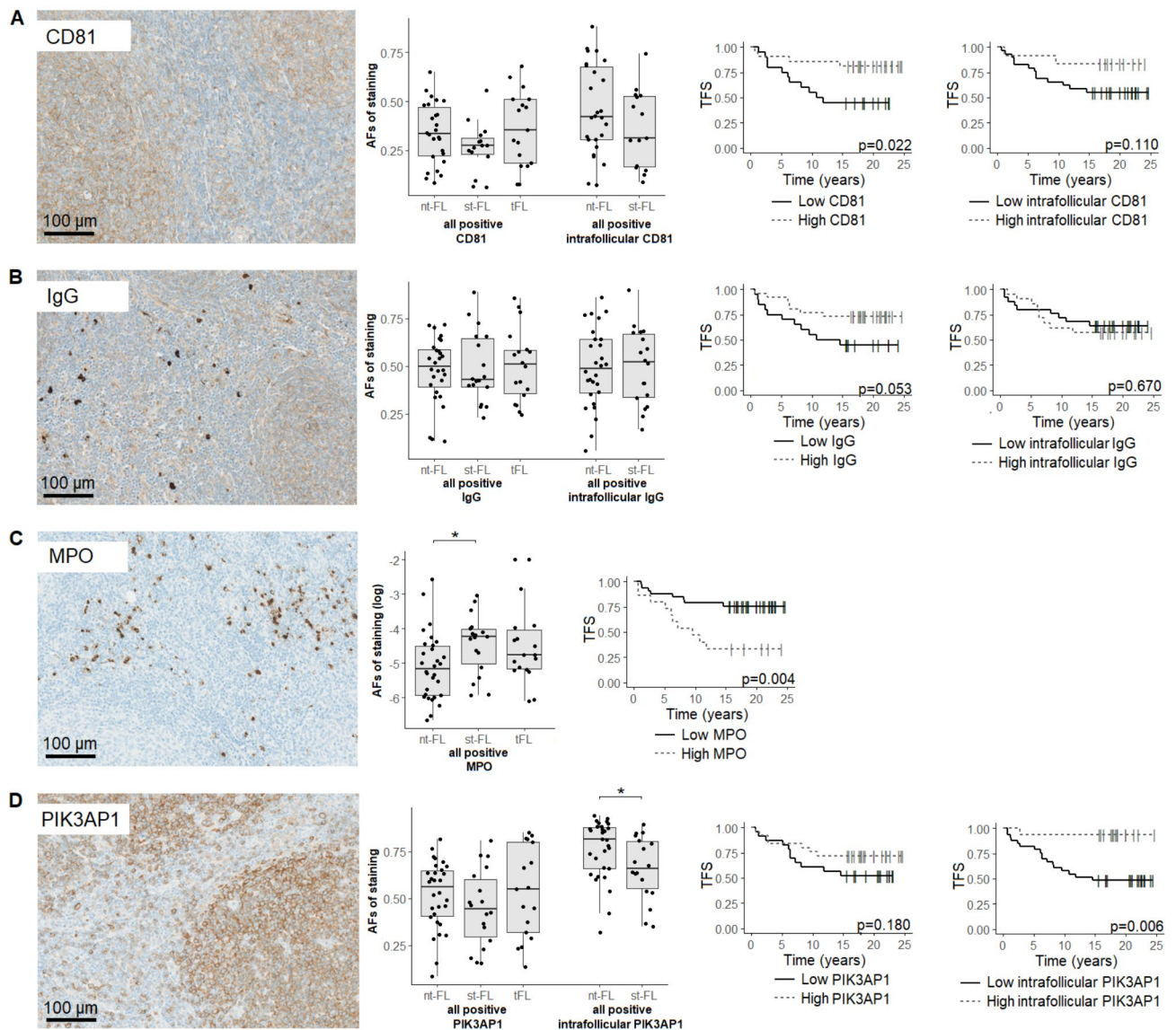


**Fig. 5.** Expression of proteins and transformation-free survival according to proteins involved in immune processes. Left: Representative images of lymphoma tissues immunohistochemically stained for (A) CD81, (B) IgG, (C) MPO, and (D) PIK3AP1. Visualized at x20. Middle: For each protein, expression levels are calculated as AFs identified by immunohistochemical staining in whole-biopsy and intrafollicular areas. Right: associations between TFS in whole-biopsy and intrafollicular expression levels, respectively, of CD81 (cutoff AF = 0.298 and AF = 0.5584), IgG (cutoff AF = 0.4447 and AF = 0.5157), MPO (cutoff AF = 0.0138), and PIK3AP1 (cutoff AF = 0.4829 and AF = 0.8485). Since MPO staining showed little or no positive staining within follicles, quantification of this marker was not performed exclusively in intrafollicular areas. \*  $p < 0.05$ ; \*\*  $p < 0.01$ ; \*\*\*  $p < 0.001$ . AF, area fraction; nt-FL, non-transforming FL; st-FL, subsequently-transforming FL; tFL, transformed FL; TFS, transformation-free survival.

routine tissue-based risk assessment of FL patients. We have previously reported that markers initially identified in the MS-based proteomics analysis were of predictive potential when assessed by immunohistochemistry on FFPE tissue<sup>13</sup>. In the initial MS-study, five proteins involved in apoptotic signaling, namely CASP3, MCL1, BAX, BCL-xL, and BCL-rambo, were investigated, showing strong predictive potential based on intratumoral expression levels. Interestingly, many of the proteins investigated in the present study showed strong correlations to one or more of these apoptotic proteins.

Furthermore, the majority of proteins showed correlations to other proteins, indicating intricate and complex interconnections between the components acting in these pathways. We divided the candidates into these five classes, although many of them may serve in more than one signaling pathway, or have several functions,

	ACTB	BID	CD11a	CD81	CDC26	CDK6	IgG	IQGAP2	MEK1	MMP9	MPO	PIK3AP1	SEPT6	SRSF1	SRSF2
ACTB															
BID	0.43 <b>0.003</b>														
CD11a	-	-													
CD81	-	-	0.44 <b>0.005</b>												
CDC26	-	0.65 <b>&lt;0.001</b>	0.44 <b>0.002</b>	-											
CDK6	0.39 <b>0.007</b>	0.66 <b>&lt;0.001</b>	-	-	0.42 <b>0.003</b>										
IgG	-	-	-	0.51 <b>0.001</b>	-	-									
IQGAP2	-0.32 <b>0.045</b>	-	-0.32 <b>0.037</b>	-	-	-	-								
MEK1	-	-0.31 <b>0.036</b>	-	-	-	-0.27 0.066	-	-							
MMP9	-	-	-	-0.40 <b>0.009</b>	-	-	-0.35 <b>0.018</b>	-	-						
MPO	0.35 <b>0.017</b>	0.28 0.055	-	-	0.35 <b>0.040</b>	0.30 <b>0.040</b>	-	-	-	0.67 <b>&lt;0.001</b>					
PIK3AP1	-	0.35 <b>0.018</b>	-	-	-	0.44 <b>0.002</b>	-	-	-	-	-				
SEPT6	-	0.37 <b>0.011</b>	0.35 <b>0.015</b>	0.35 <b>0.027</b>	0.40 <b>0.005</b>	0.31 <b>0.032</b>	-	-	-	-	-	-			
SRSF1	0.27 0.071	0.69 <b>&lt;0.001</b>	0.26 0.079	-	0.67 <b>&lt;0.001</b>	0.55 <b>&lt;0.001</b>	-	-	-0.35 <b>0.016</b>	-	0.37 <b>0.011</b>	0.43 <b>0.003</b>	0.34 <b>0.018</b>		
SRSF2	-	-0.45 <b>0.002</b>	-0.52 <b>&lt;0.001</b>	-	-0.42 <b>0.004</b>	-0.28 0.064	-	0.42 <b>0.007</b>	0.53 <b>&lt;0.001</b>	-	-0.37 <b>0.012</b>	-	-	-0.43 <b>0.003</b>	

**Table 3.** Intercorrelations between biomarkers Top, correlation coefficient  $\rho$ ; bottom, p-value. The level of significance for the entire paper is defined in the methods section as  $p < 0.05$ .

	ACTB	BID	CD11a	CD81	CDC26	CDK6	IgG	IQGAP2	MEK1	MMP9	MPO	PIK3AP1	SEPT6	SRSF1	SRSF2
Female gender	-	0.30 <b>0.041</b>	-	-	0.27 <b>0.055</b>	-	-	-	-	-	-	0.34 <b>0.019</b>	-	-	-
Age	-	-	-	-	-	-	-	-	-	-0.35 <b>0.014</b>	-0.29 <b>0.048</b>	-	-	-	-
Ann Arbor stage	-	-	-	-	-	0.42 <b>0.003</b>	-	-	-	0.47 <b>&lt;0.001</b>	-	-	-0.29 <b>0.048</b>	-	-
FLIPI	0.30 <b>0.051</b>	-	-	-	-	0.33 <b>0.028</b>	-	-	-	0.46 <b>0.002</b>	-	-	-	-	-
LDH levels	-	-	-0.30 <b>0.047</b>	-	-	-	-	-	-	-	-	-	-	-	-
Bone marrow involvement	-	-	-0.33 <b>0.036</b>	-0.49 <b>0.002</b>	-	-	-0.43 <b>0.005</b>	-	-	0.48 <b>0.001</b>	-	-	-0.29 <b>0.059</b>	-	-
Lymphocyte counts	-	-	-	-	-	-	-	-	-	-0.38 <b>0.014</b>	-	-	-	-	-
Hgb levels	-	-	-	-	-	0.31 <b>0.037</b>	-	-	-	-	-	-	-	-	-
FL grade	-	-	-	-	-	-	-	-	-	-	0.34 <b>0.017</b>	-	-	-	-

**Table 4.** Correlations between biomarkers and clinicopathological features Top, correlation coefficient  $\rho$ ; bottom, p-value. FLIPI, follicular lymphoma international prognostic index; Hgb, hemoglobin; LDH, lactate dehydrogenase. The level of significance for the entire paper is defined in the methods section as  $p < 0.05$ .

thus influencing more than one pathway. While ACTB has traditionally been regarded as an endogenous housekeeping gene, its expression is closely associated with a variety of cancers. Accumulating evidence indicates that ACTB is deregulated in several solid cancers, and in hematology it was previously associated to drug resistance in mantle cell lymphoma<sup>22–24</sup>. ACTB is generally upregulated in tumor cells and tissues, where abnormal expression and polymerization of ACTB may promote cancer cell motility and invasiveness via the resulting changes to the cytoskeleton<sup>22,24,25</sup>. Furthermore, mounting evidence implicates the actin cytoskeleton to play a key role as a sensor, mediator, and regulator of apoptosis<sup>26</sup>. Indeed, in the present study, we found a strong correlation of ACTB to the previously investigated apoptotic markers as well as to BID, a death agonist that

heterodimerizes with either agonist BAX or antagonist BCL2, and thus regulates apoptosis<sup>27</sup>. BID has previously been described in colon and gastric cancer<sup>28–31</sup>. In addition, Debernardi et al. reported that the initiation of apoptotic pathways in Burkitt lymphoma cells required cleavage of the BID protein as well as activation of two other apoptogenic proteins, BAK and BAX, which were both also identified as upregulated in st-FL samples in our initial MS-based proteomics study<sup>13,32</sup>. While only correlated to BCL-xL expression, another interesting protein in the context of apoptosis and the cytoskeleton is MMP9. MMPs represent a large family of enzymes that degrade most extracellular matrix components, acting also in the field of cancer progression, tumor growth, and metastasis<sup>33,34</sup>. In FL and other lymphomas, high MMP9 expression has previously been correlated with tumor grade, invasive behavior, and inferior survival rates<sup>35–40</sup>. MMP9 especially has also been associated with active neovascularization and angiogenesis<sup>33,34</sup>. Moreover, MMPs acts in evading programmed cell death by interfering with the induction of apoptosis in malignant cells<sup>33</sup>. Mounting evidence supports the view that extracellular proteinases, such as MMPs, mediate many of the changes in the microenvironment during tumor progression. Tumor progression depends on a highly regulated and complex remodeling of the TME through processes of cleavage, action of adhesion molecules and growth factors, as well as modulation of the function of cytokines and chemokines surrounding the infiltrating immune cells; this results in an immunoregulatory function, affecting their intricate interaction in and around the tumor cells<sup>33,34</sup>. In relation to the TME, we found a negative correlation between MMP9 and CD81, which was also indicated by inferior TFS rates associated with high MMP9 levels and low CD81 levels. CD81 serves in B cell receptor signaling, where CD19 functions as the dominant signaling component alongside CD21, CD81 and CD225<sup>41,42</sup>. In solid tumors, CD81 regulates key processes such as tumor growth, migration and invasion<sup>43</sup>. Interestingly, CD81 have been shown to both promote and to suppress tumor growth, and, correspondingly, association to prognosis has been divergent across different cancers. For example, low expression of CD81 had higher metastatic potential in hepatocellular carcinoma cell lines, inactivation of CD81 conferred growth and survival advantages to gastric tumors, and low CD81 expression in bladder cancer was associated with inferior prognoses requiring closer surveillance and more aggressive treatment<sup>43–46</sup>. In contrast, overexpression of CD81 in melanoma cell lines significantly increased their invasive potential<sup>43,47</sup>. The role of CD81 in hematological malignancies has been less explored. However, in acute myeloid leukemia, high numbers of CD81-positive blasts were correlated with inferior prognosis<sup>48,49</sup>. CD81 expression in FL has previously been characterized, however, with no information on association to transformation nor prognosis<sup>50–52</sup>. Notably, Lou et al. found high expression of CD81 in germinal center B cells, with positive expression in the majority of B cell lymphomas, including FL and DLBCL<sup>52</sup>. We also found expression levels of IQGAP2 to be lower in st-FL samples than nt-FL samples. Expression of the Rho-GTPase-associated protein IQGAP2 is reduced and plays a tumor suppressor role in many solid cancers. The protein interacts with components of the cytoskeleton and cell adhesion molecules, among others, and it acts as a putative Rac Family Small GTPase 1 (RAC1)/cell division cycle 42 (CDC42) effector protein<sup>53,54</sup>. Other proteins driving cell cycle, including CDC26, CDK6, and SRSF1, were also analyzed in the present study, and these were also correlated to several apoptotic markers. Previously, CDK6 expression has been shown to be commonly altered with enhanced kinase activity in hematopoietic malignancies, and it has been identified as an adverse prognostic factor in DLBCL<sup>55,56</sup>. SRSF1, a splicing factor resulting from the potent proto-oncogene *SRSF1*, also plays a role in proteolysis, nucleotide excision repair, the p53-pathway, and apoptosis, among others<sup>57</sup>. It has been reported that BCL-x is a known target of SRSF1 into the isoforms BCL-xL and BCL-xS, but the detailed regulatory mechanisms are not fully elucidated<sup>58–60</sup>. Analyses have shown that high expression of the proto-oncogene was correlated with poor prognosis in hematological malignancies<sup>61</sup>. Taken together, the interplay between several of the investigated proteins suggests that interaction between comprehensive mechanisms of cell death, the composition of the cytoskeletal and extracellular matrix, the cell cycle, and immune cell infiltrates is important in follicular lymphoma biology. Our results indicate that additional mechanistic studies to explore further these cellular pathways and identified targets are warranted.

## Conclusion

In conclusion, this study sheds light on the intricate biology of FL and the underlying mechanisms of HT, a significant challenge in the clinical management of this lymphoma. The reported differences in proteins acting in five pathway classes, spanning critical cellular pathways, have provided new insights in FL tumor biology, and have highlighted protein expression in tumor and bystander cells with potential value as predictive markers for FL transformation. The interplay between these proteins and their correlations with apoptotic markers underscore the complexity of FL biology. Notably, this underlines the importance of the TME in FL, suggesting that it may hold the key to novel therapeutic targets.

## Data availability

Data may be shared upon reasonable request to the corresponding authors.

Received: 18 September 2024; Accepted: 28 November 2024

Published online: 02 December 2024

## References

1. Friedberg, J. W. Update on follicular lymphoma. *Hematol. Oncol.* **41** (Suppl 1(Suppl 1), 43–47 (2023).
2. Swerdlow, S. H. et al. The 2016 revision of the World Health Organization classification of lymphoid neoplasms. *Blood* **127** (20), 2375–2390 (2016).
3. Wang, X. et al. Single-cell profiling reveals a memory B cell-like subtype of follicular lymphoma with increased transformation risk. *Nat. Commun.* **13** (1), 6772 (2022).

4. Kridel, R. et al. Histological Transformation and Progression in Follicular Lymphoma: a clonal evolution study. *PLoS Med.* **13** (12), e1002197 (2016).
5. Wagner-Johnston, N. D. et al. Outcomes of transformed follicular lymphoma in the modern era: a report from the National LymphoCare Study (NLCS). *Blood* **126** (7), 851–857 (2015).
6. Sarkozy, C. et al. Risk factors and outcomes for patients with follicular Lymphoma who had histologic Transformation after response to First-Line Immunochemotherapy in the PRIMA Trial. *J. Clin. Oncol.* **34** (22), 2575–2582 (2016).
7. Beck Enemark, M. et al. PD-1 expression in Pre-treatment Follicular Lymphoma predicts the risk of subsequent high-Grade Transformation. *Onco Targets Ther.* **14**, 481–489 (2021).
8. Blaker, Y. N. et al. The tumour microenvironment influences survival and time to transformation in follicular lymphoma in the Rituximab era. *Br. J. Haematol.* **175** (1), 102–114 (2016).
9. Dave, S. S. et al. Prediction of survival in follicular lymphoma based on molecular features of tumor-infiltrating immune cells. *N Engl. J. Med.* **351** (21), 2159–2169 (2004).
10. Smeltzer, J. P. et al. Pattern of CD14+ follicular dendritic cells and PD1+ T cells independently predicts time to transformation in follicular lymphoma. *Clin. Cancer Res.* **20** (11), 2862–2872 (2014).
11. Wahlin, B. E. et al. A unifying microenvironment model in follicular lymphoma: outcome is predicted by programmed death-1-positive, regulatory, cytotoxic, and helper T cells and macrophages. *Clin. Cancer Res.* **16** (2), 637–650 (2010).
12. Andersen, M. H. Tumor microenvironment antigens. *Semin Immunopathol.* **45** (2), 253–264 (2023).
13. Enemark, M. B. H. et al. Proteomics identifies apoptotic markers as predictors of histological transformation in patients with follicular lymphoma. *Blood Adv.* **7** (24), 7418–7432 (2023).
14. Arboe, B. et al. The Danish National Lymphoma Registry: Coverage and Data Quality. *PLoS One.* **11** (6), e0157999 (2016).
15. Arboe, B. et al. Danish National Lymphoma Registry. *Clin. Epidemiol.* **8**, 577–581 (2016).
16. Enemark, M. B. et al. Tumor-tissue expression of the Hyaluronic acid receptor RHAMM predicts histological Transformation in Follicular Lymphoma patients. *Cancers (Basel)* ;**14**(5). (2022).
17. Madsen, C. et al. High intratumoral expression of vimentin predicts histological transformation in patients with follicular lymphoma. *Blood Cancer J.* **9** (4), 35 (2019).
18. Madsen, C. et al. Real world data on histological transformation in patients with follicular lymphoma: incidence, clinicopathological risk factors and outcome in a nationwide Danish cohort. *Leuk. Lymphoma.* **61** (11), 2584–2594 (2020).
19. Monrad, I. et al. Glycolytic biomarkers predict transformation in patients with follicular lymphoma. *PLoS One.* **15** (5), e0233449 (2020).
20. Enemark, M. B. H. et al. IDO1 protein is expressed in Diagnostic biopsies from both follicular and transformed follicular patients. *Int. J. Mol. Sci.* ;**24**(8). (2023).
21. Kumar, E. A., Okosun, J. & Fitzgibbon, J. The Biological basis of histologic Transformation. *Hematol. Oncol. Clin. North. Am.* **34** (4), 771–784 (2020).
22. Guo, C., Liu, S., Wang, J., Sun, M. Z. & Greenaway, F. T. ACTB in cancer. *Clin. Chim. Acta.* **417**, 39–44 (2013).
23. Weinkauff, M. et al. 2-D PAGE-based comparison of proteasome inhibitor bortezomib in sensitive and resistant mantle cell lymphoma. *Electrophoresis* **30** (6), 974–986 (2009).
24. Gu, Y. et al. A pan-cancer analysis of the prognostic and immunological role of  $\beta$ -actin (ACTB) in human cancers. *Bioengineered* **12** (1), 6166–6185 (2021).
25. Bunnell, T. M., Burbach, B. J., Shimizu, Y. & Ervasti, J. M.  $\beta$ -Actin specifically controls cell growth, migration, and the G-actin pool. *Mol. Biol. Cell.* **22** (21), 4047–4058 (2011).
26. Desouza, M., Gunning, P. W. & Stehn, J. R. The actin cytoskeleton as a sensor and mediator of apoptosis. *Bioarchitecture* **2** (3), 75–87 (2012).
27. Hapko, L., Strasser, A. & Cory, S. BH3-only proteins in apoptosis at a glance. *J. Cell. Sci.* **125** (Pt 5), 1081–1087 (2012).
28. Gryko, M. et al. The expression of Bcl-2 and BID in gastric cancer cells. *J. Immunol. Res.* **2014**, 953203 (2014).
29. Rupnarain, C., Dlamini, Z., Naicker, S. & Bhoola, K. Colon cancer: genomics and apoptotic events. *Biol. Chem.* **385** (6), 449–464 (2004).
30. Gu, Q. et al. Activation of the caspase-8/Bid and Bax pathways in aspirin-induced apoptosis in gastric cancer. *Carcinogenesis* **26** (3), 541–546 (2005).
31. Sinicrope, F. A. et al. Proapoptotic bad and bid protein expression predict survival in stages II and III colon cancers. *Clin. Cancer Res.* **14** (13), 4128–4133 (2008).
32. Debernardi, J., Hollville, E., Lipinski, M., Wiels, J. & Robert, A. Differential role of FL-BID and t-BID during verotoxin-1-induced apoptosis in Burkitt's lymphoma cells. *Oncogene* **37** (18), 2410–2421 (2018).
33. Kessenbrock, K., Plaks, V. & Werb, Z. Matrix metalloproteinases: regulators of the tumor microenvironment. *Cell* **141** (1), 52–67 (2010).
34. Niland, S., Riscanevo, A. X. & Eble, J. A. Matrix metalloproteinases shape the Tumor Microenvironment in Cancer Progression. *Int. J. Mol. Sci.* ;**23**(1). (2021).
35. Sakata, K. et al. Expression of matrix metalloproteinase 9 is a prognostic factor in patients with non-hodgkin lymphoma. *Cancer* **100** (2), 356–365 (2004).
36. Hazar, B. et al. Prognostic value of matrix metalloproteinases (MMP-2 and MMP-9) in Hodgkin's and Non-hodgkin's lymphoma. *Int. J. Clin. Pract.* **58** (2), 139–143 (2004).
37. Kossakowska, A. E., Urbanski, S. J. & Janowska-Wieczorek, A. Matrix metalloproteinases and their tissue inhibitors - expression, role and regulation in human malignant non-hodgkin's lymphomas. *Leuk. Lymphoma.* **39** (5–6), 485–493 (2000).
38. Fruchon, S. et al. Involvement of the Syk-mTOR pathway in follicular lymphoma cell invasion and angiogenesis. *Leukemia* **26** (4), 795–805 (2012).
39. Zhang, Q. & Wang, M. Identification of hub genes and key pathways Associated with Follicular Lymphoma. *Contrast Media Mol. Imaging.* **2022**, 5369104 (2022).
40. Zhou, Y. et al. Low CCL19 expression is associated with adverse clinical outcomes for follicular lymphoma patients treated with chemoimmunotherapy. *J. Transl. Med.* **19** (1), 399 (2021).
41. Del Nagro, C. J. et al. CD19 function in central and peripheral B-cell development. *Immunol. Res.* **31** (2), 119–131 (2005).
42. Wang, K., Wei, G. & Liu, D. CD19: a biomarker for B cell development, lymphoma diagnosis and therapy. *Exp. Hematol. Oncol.* **1** (1), 36 (2012).
43. Vences-Catalán, F. et al. CD81 as a tumor target. *Biochem. Soc. Trans.* **45** (2), 531–535 (2017).
44. Mazzocca, A., Liotta, F. & Carloni, V. Tetraspanin CD81-regulated cell motility plays a critical role in intrahepatic metastasis of hepatocellular carcinoma. *Gastroenterology* **135** (1), 244–256e241 (2008).
45. Yoo, T. H., Ryu, B. K., Lee, M. G. & Chi, S. G. CD81 is a candidate tumor suppressor gene in human gastric cancer. *Cell. Oncol. (Dordr).* **36** (2), 141–153 (2013).
46. Lee, M. S. et al. Prognostic significance of CREB-Binding protein and CD81 expression in primary high Grade Non-muscle invasive bladder Cancer: identification of novel biomarkers for bladder Cancer using antibody microarray. *PLoS One.* **10** (4), e0125405 (2015).
47. Hong, I. K. et al. The tetraspanin CD81 protein increases melanoma cell motility by up-regulating metalloproteinase MT1-MMP expression through the pro-oncogenic akt-dependent Sp1 activation signaling pathways. *J. Biol. Chem.* **289** (22), 15691–15704 (2014).

48. Boyer, T. et al. Tetraspanin CD81 is an adverse prognostic marker in acute myeloid leukemia. *Oncotarget* **7** (38), 62377–62385 (2016).
49. Floren, M. & Gillette, J. M. Acute myeloid leukemia: therapy resistance and a potential role for tetraspanin membrane scaffolds. *Int. J. Biochem. Cell. Biol.* **137**, 106029 (2021).
50. Cardoso, C. C. et al. The importance of CD39, CD43, CD81, and CD95 expression for differentiating B cell lymphoma by flow cytometry. *Cytometry B Clin. Cytom.* **94** (3), 451–458 (2018).
51. Espasa, A. et al. Flow cytometric expression of CD71, CD81, CD44 and CD39 in B cell lymphoma. *Scand. J. Clin. Lab. Invest.* **81** (5), 413–417 (2021).
52. Luo, R. F. et al. CD81 protein is expressed at high levels in normal germinal center B cells and in subtypes of human lymphomas. *Hum. Pathol.* **41** (2), 271–280 (2010).
53. Hedman, A. C., Smith, J. M. & Sacks, D. B. The biology of IQGAP proteins: beyond the cytoskeleton. *EMBO Rep.* **16** (4), 427–446 (2015).
54. Song, F., Dai, Q., Grimm, M. O. & Steinbach, D. The antithetic roles of IQGAP2 and IQGAP3 in cancers. *Cancers (Basel)* ;**15**(4). (2023).
55. Su, H., Chang, J., Xu, M., Sun, R. & Wang, J. CDK6 overexpression resulted from microRNA-320d downregulation promotes cell proliferation in diffuse large B-cell lymphoma. *Oncol. Rep.* **42** (1), 321–327 (2019).
56. Nebenfuhr, S., Kollmann, K. & Sxcl, V. The role of CDK6 in cancer. *Int. J. Cancer.* **147** (11), 2988–2995 (2020).
57. Lo Giudice, A. et al. The clinical role of SRSF1 expression in Cancer: a review of the current literature. *Appl. Sci.* **12** (5), 2268 (2022).
58. Lv, Y. et al. SRSF1 inhibits autophagy through regulating Bcl-x splicing and interacting with PIK3C3 in lung cancer. *Signal. Transduct. Target. Ther.* **6** (1), 108 (2021).
59. Moore, M. J., Wang, Q., Kennedy, C. J. & Silver, P. A. An alternative splicing network links cell-cycle control to apoptosis. *Cell* **142** (4), 625–636 (2010).
60. Wang, Y. et al. The splicing factor RBM4 controls apoptosis, proliferation, and migration to suppress tumor progression. *Cancer Cell.* **26** (3), 374–389 (2014).
61. Salifu, S. P. & Doughan, A. New clues to prognostic biomarkers of four hematological malignancies. *J. Cancer.* **13** (8), 2490–2503 (2022).

## Acknowledgements

The authors thank Hanh Pham Hansen, Department of Pathology, Aarhus University Hospital for her excellent technical assistance. The research was funded with grants from Department of Clinical Medicine, Aarhus University, the Karen Elise Jensen Foundation, Merchant Einar Willumsen's Memorial Foundation, the Danish Lymphoma Group, a donation from Peter and Alice Madsen, Knud and Edith Eriksen's Memorial Foundation, Eva and Henry Fränkel's Memorial Foundation, Raimond and Dagmar Ringgård-Bohn's Foundation, Butcher Max Wörzner and wife Wörzner's Memorial Grant, Master Carpenter Jørgen Holm and wife Elisa f. Hansen's Memorial Grant, A.P. Møller Foundation for the Advancement of Medical Sciences, Dagmar Marshall's Foundation, and Farmer of "Ølufgård" Peder Nielsen Kristensens Memorial Foundation.

## Author contributions

MHE, BH, and ML conceptualized the study and study design. MHE, KW, EFS, MDA, LMH, KLL, CM, TLP, SHD, BH, and ML executed the experiments and statistical analyses. TLP and SHD revised the pathological diagnoses. MHE and CM did clinical data acquisition. All authors contributed to data interpretation. MHE and ML wrote the initial manuscript draft. All authors critically reviewed the manuscript and approved the final version.

## Declarations

### Conflict of interest

BH holds shares in Novo Nordisk A/S and Genmab A/S. Novo Nordisk A/S and Genmab A/S had no influence on the study design, analyses and reporting of results. All other authors declare no relevant competing financial interests.

## Additional information

**Supplementary Information** The online version contains supplementary material available at <https://doi.org/10.1038/s41598-024-81693-4>.

**Correspondence** and requests for materials should be addressed to M.L.

**Reprints and permissions information** is available at [www.nature.com/reprints](http://www.nature.com/reprints).

**Publisher's note** Springer Nature remains neutral with regard to jurisdictional claims in published maps and institutional affiliations.

**Open Access** This article is licensed under a Creative Commons Attribution-NonCommercial-NoDerivatives 4.0 International License, which permits any non-commercial use, sharing, distribution and reproduction in any medium or format, as long as you give appropriate credit to the original author(s) and the source, provide a link to the Creative Commons licence, and indicate if you modified the licensed material. You do not have permission under this licence to share adapted material derived from this article or parts of it. The images or other third party material in this article are included in the article's Creative Commons licence, unless indicated otherwise in a credit line to the material. If material is not included in the article's Creative Commons licence and your intended use is not permitted by statutory regulation or exceeds the permitted use, you will need to obtain permission directly from the copyright holder. To view a copy of this licence, visit <http://creativecommons.org/licenses/by-nc-nd/4.0/>.

© The Author(s) 2024